MATEC Web of Conferences **18**, 01012 (2014)
DOI: 10.1051/matecconf/ 20141801012

AUGMENTATION OF THE CRITICAL HEAT FLUX IN WATER-Al_2O_3, WATER-TiO_2 AND WATER-Cu NANOFLUIDS

Janusz T. Cieśliński[1] , **Katarzyna Krygier**[1]

[1]Gdansk University of Technology, Narutowicza 11/12, 80-233 Gdansk, Poland
E-mail : jcieslin@pg.gda.pl

Keywords: *pool boiling, nanofluid, CHF*

1. INTRODUCTION

Nanofluids as new category of fluids may revolutionize heat transfer technology. Nanofluid it is a mixture/suspension of the base liquid and nanoparticles with a size below 100 nm [1]. Conflicting results as far as effect of nanoparticles on the pool boiling heat transfer performance have been reported [2,3]. However, the data published in the open literature show, that application of nanofluids results in distinct increase of critical heat flux – even almost three times compared to the boiling of pure, base liquid. It seems that You et al. [4] were the first that investigated CHF phenomenon with nanofluids. They demonstrated that the CHF of water-Al_2O_3 water nanofluids - while boiling on a flat plate, was about 200% higher than that for pure water when the particle volume fraction exceeded 0.005 g/L. Furthermore, they concluded that the unusual CHF enhancement with nanofluids could not be explained by any existing model of CHF. Vassallo et al. [5] conducted experiments on the NiCr wire that confirms the increasing CHF of nanofluids. They examined the boiling characteristics of silica–water nanofluids with 0.5% volume concentration and observed a thick SiO_2 coating (0.15–0.2 mm) on the wire, suggesting that there was a surface interaction between the nanoparticles and the wire. Dinh et al. [6] observed CHF increase during boiling of water-Al_2O_3 nanofluid on horizontal plates covered with titanium films (460 nm). They postulated that CHF increase results from two premises: creation of nanocoating and extraordinary ability of nanofluids to wet the heater called super-spreading. Moreno et al. [7] established that at saturation temperature T_{sat}=60°C, the maximum CHF enhancement as compared to the predicted Zuber's CHF evaluated at an equivalent saturation temperature is ~180% for water-Al_2O_3 nanofluids and ~240% for water-ZnO nanofluids. The dispersion of Al_2O_3 nanoparticles in various ethylene glycol solutions is also found to enhance CHF by as much as ~130%. Bang and Chang [8] studied the pool boiling heat transfer of water-Al_2O_3 nanofluids on a flat plate heater, and measured the surface roughness of the heater before and after the pool boiling experiment. They reported that the CHF was enhanced in both horizontal and vertical pool boiling. In addition, using surface roughness data, they hypothesized that the change in CHF performance was related to the change in the surface characteristics with the deposition of nanoparticles. However, these studies could not precisely determine the reason for the outstanding enhancement of the CHF using nanofluids, and simply conjectured that the effect was related to the surface coating of nanoparticles. Milanova and Kumar [9] reported that nanosilica suspension increases the CHF 3 times compared to water while boiling on wire. Jackson et al. [10] studied boiling of water-Au nanofluid on circular plate. They established CHF 1.5 times higher than for pure water. Kim et al. [11,12] investigated boiling of water-based nanofluids with titania and alumina nanoparticles on NiCr an Ti wires. The results showed that the nanofluids significantly (up to 170%) enhanced CHF compared to that of pure water. Kim et al. [13,14] observed CHF enhancement during water-Al_2O_3, water-ZrO_2 and water-SiO_2 nanofluids on flat horizontal plate and wires. They attributed CHF enhancement to contact angle reduction. Kashinath [15] conducted experiments in order to check the effect of heater size, pressure, heater orientation and effect of anti-freeze addition on CHF of water and glycol based nanofluids using Al_2O_3 nanoparticles. Nanofluids have shown about ~ 180 - 200% enhancement in CHF values. The effect of heater was examined using three different sized heaters. Maximum enhancement of ~190% was achieved for a 1×1 cm heater. The effect of pressure on CHF was investigated by testing nanofluids at three pressures. Maximum enhancement of ~240% increase in CHF was observed at the lowest pressure tested. Surface orientation effect on CHF tested for a 2×2 cm heater at five orientations revealed about ~120% enhancement over the CHF obtained using Zuber's correlation at an orientation of 150°. Two commercially used antifreezes, ethylene glycol and propylene glycol, were used to study the effect of anti-freeze addition to nanofluids. Alumina-water nanofluid of 0.025 g/L concentration mixed with the antifreezes at five compositions by volume showed a maximum enhancement of ~120% for ethylene glycol and ~70% for propylene glycol. Milanova et al. [16] used water based nanofluids with SiO_2, CeO_2 and Al_2O_3 nanoparticles. They stated that amorphous oxides (SiO_2) are generally more disordered and less closely packed compared to the crystalline oxides such as CeO_2 and Al_2O_3. The arrangement of the atoms within the unit cell and the layer of water molecules at the surface possibly influence the CHF. The boiling regime is further extended to higher heat flux when there is agglomeration on the wire. This agglomeration allows high heat transfer through interagglomerate pores, resulting in a nearly 3-fold increase in CHF. This deposition occurs for the charged 10 nm silica particle, and was not seen for other oxide particles. Kim et al. [17] determined that addition of TiO_2 resulted in 200% of CHF during boiling on a NiCr wire compared to that of pure water by increasing nanoparticle concentration. Kim H. and Kim D. [18] noticed CHF enhancement during boiling of water-TiO_2, water-Al_2O_3, water-SiO_2 nanofluids while no augmentation of CHF was observed for water-Ag nanofluid. They concluded that the significant CHF enhancement is a consequence of not only increased surface wettability but also improved capillarity due to the surface deposition of nanoparticles. Kim et al. [19] established that CHF is degraded during boiling of nanofluids on nanoparticle-coated heating surface because nanoparticles may clog micro-passes supplying the bulk liquid to the heating surface by capillary wicking. Liu et al. [20] studied pool boiling of water–CuO nanofluid on horizontal copper plate with microgrooves. The grooves were of 0.5 mm wide and 0.8 mm deep. The gap between the two grooves was 0.5 mm. The experiments were conducted under four operating pressures of 7.4 kPa, 20 kPa, 31.2 kPa and 100 kPa. CHF enhancement strongly depends on operating pressure. For optimum nanoparticle concentration of 1% and operating pressure of 7.4

Article available at http://www.matec-conferences.org or http://dx.doi.org/10.1051/matecconf/20141801012

kPa CHF was about two times higher than for pure water. Coursey and Kim [21] investigated boiling of water-Al_2O_3 and ethanol-Al_2O_3 nanofluids on circular plates made of glass, Au and Cu. They noticed that the greater concentrations led to modest (up to 37%) increase in the CHP. Liu and Liao [22] stated that the very thin nanoparticle sorption layer caused a decrease in solid-liquid contact angle on the heating surface which lead to and increase of CHF. Milanova and Kumar [23] determined that when there was no nanoparticle deposition on the wire, the nanofluid water-SiO_2 increased CHF by about 50% regardless of pH of the base liquid (3, 4, 7, 10) or particle size (10-20 nm). Golubovic et al. [24] revealed that the increase of nanoparticle concentration in the nanofluid increases the CHF up to a certain point, after which further increase does not effect CHF. They believe in hydrodynamic nature of CHF. Jo et al. [25] established that CHF were significantly enhanced for different nanoparticle sizes and concentrations. The CHF of nanofluids was increased as the size of the nanoparticles decreased. On the other hand, nanoparticle concentration value showing the maximum CHF had a critical value. Kumar and Milanova [26] showed that CHF is a strong function of the relaxation of the surface tension of the nanofluid, i.e. the difference in the surface tension between the nanofluid and surfactant solution. The maximum enhancement in CHF is nearly four times for a surfactant to CNT concentration ratio of 1:5. Kim H. and Kim M. [27] reported outstanding CHF improvement during boiling of water-TiO_2, water-Al_2O_3 and water-SiO_2 nanofluids on horizontal wire. The final effect is strongly dependent on the kind of nanoparticles, as well as its concentration (10–5-10–1 vol.%). Park et al. [28] stressed that CHF improvement results from CNTs deposition and formation of a thin film on the surface. Because of this deposition, the probability of forming large vapor blanket by bubbles at high heat flux decreased and consequently, the CHF increased. Kim et al. [29] established that the quenching behavior in nanofluids is nearly identical to that in pure water. However, it was found that some nanoparticles accumulate on the sphere surface, which results in destabilization of the vapor film in subsequent tests with the same sphere, thus greatly accelerating the quenching process. Kathiravan et al. [30] found that CHF increased with nanoparticle concentration increase during boiling of water-Cu nanofluid on 30 mm square flat plate. However, addition of surfactant (SDS) to nanofluid resulted in dramatic CHF degradation. Kwark et al. [31] carried out experiments with boiling of water-Al_2O_3, water-CuO and water-diamond nanofluids. They postulated that there is an optimal nanocoating thickness/structure which can produce the maximum CHF enhancement. Furthermore, it seems that boiling itself appears to be the mechanism responsible for the nanoparticle coating formation as the vapor bubbles' microlayer evaporate. Kwark et al. [32,33] conducted experiments with boiling of pure water on a plate covered with nanocoating created during ethanol-Al_2O_3 nanofluid. When tested in water, these nanocoatings had ability to enhance CHF. Kwark et al. showed that pool boiling performance of pure water on Al_2O_3 nanoparticle coated flat heaters is dependent on such parameters as operating pressure, heater size and heater orientation. They postulated that the better wettability in the nanocoating, especially its ability to continuously rewet the base of the growing bubbles, was the main cause of CHF enhancement. Liu et al. [34] experimentally demonstrated that pressure significantly influences CHF of CNT nanofluids. They postulated that CHF depends on the thickness and the wettability area of the thin liquid microlayer underneath vapor bubble. If the CNT nanoparticles accumulated in the liquid microlayer during the boiling process the CHF can be increased due to that the increases of both the effective thermal conductivity and the wettability area of the thin liquid microlayer. At the atmospheric pressure, the effects of the accumulation of CNTs in the thin liquid microlayer may be weak due to that it is difficult for nanoparticles to enter into the liquid microlayer. However, in the sub-atmospheric pressures, the effects of the accumulation may be stronger than that in the atmospheric pressure, so the heat transfer enhancement would increase with the decrease of the pressure. Kim et al. [35] recorded significant CHF enhancement during boiling of alumina (Al_2O_3) and titania (TiO_2) nanofluids on heated disk. It is supposed that the nanoparticle layer increases the stability of the evaporating microlayer underneath a bubble growing on a heated surface and thus the irreversible growth of a hot/dry spot is inhibited even at a high wall superheat, resulting in the CHF enhancement observed when boiling nanofluids. Park et al. [36] used graphene and graphene-oxide nanosheets (GON) as the additives in nanofluids and they recorded outstanding CHF improvement, especially for water-GON nanofluid (172%). As a potential explanation Park et al. suggest that application of GON results in building up a characteristically ordered porous surface structure due to its own self-assembly characteristics resulting in a geometrically changed critical Rayleigh-Taylor instability wavelength. Truong et al. [37] determined that nanofluids can further increase pool boiling CHF by forming a porous deposition on the heated surface. They tested three water-based nanofluids (diamond, zinc oxide and alumina) to modify sandblasted stainless steel 316 plate heaters via boiling induced deposition. The pool boiling CHF of these pre-coated heaters increased by up to 35% with respect to that of the bare, sandblasted heaters. The enhancements are highest for alumina and zinc oxide nanofluids. Kathiravan et al. [38] observed CHF increase with concentration of silver nanoparticles suspended in water as well as in water-surfactant base liquid. Park et al. [39] used xGnPs and xGnPs oxide to prepare experimental nanofluids. The critical heat flux (CHF) of nanofluids when boiled over a NiCr wire increased with increasing concentrations of xGnP and xGnP oxide particles in the base fluid. They noticed that the xGnP oxide nanofluids with 0.005 vol% dispersed particle concentration had the most enhanced CHF. Although the largest CHF enhancement was observed for the nanofluid with 0.005 vol% xGnP oxide, no reduction was observed in the contact angle. Lee et al. [40] proposed the magnetic nanofluids (or an engineered colloidal suspension of magnetite nanoparticles in water) as the new coolant material to overcome the shortcomings of nanofluids, and the flow boiling CHF characteristics of magnetic nanofluids was quantified. They observed significant amount of CHF enhancement. Lee et al. [41] described the effect of high pressure on CHF enhancement using water-based nanofluids. They found that the CHF was generally increased with increasing the system pressure. Hiswankar and Kshirsagar [42] studied pool boiling with water based nanofluid and ZnO nanoparticles. The results showed that the water-based nanofluids significantly enhanced CHF compared to that of pure water. The CHF values of the ZnO nanofluids were enhanced from approximately 70% to 80% of pure water. It was found that a sizable layer of nanoparticle deposits were formed on heater surface. Park et al. [43] studied the Ag, Cu, and Al_2O_3 nanofluids produced by the electrical explosion of wire in liquids (EEWL). The EEWL as physical method has many advantages such as high-purity nanofluids production without surfactants (non-toxic, in contrast to chemical method), control of oxidation of nanoparticles surface, and spherical nanoparticle production. They performed pool boiling experiments to characterize the CHF enhancement using Ag, Cu and Al_2O_3 nanofluids. The heater surface contained deposited nanoparticles that formed nano/microstructures. Build-up of the nanoparticles on the heater

surface occurred during nucleate boiling, which decreased the contact angle of heater surface. The improving of surface wettability contributed to the CHF enhancement. Kole et al. [44] studied the pool boiling characteristics of copper-distilled water nanofluids which were determined employing cylindrical heater surfaces of three different materials, namely, copper, brass and aluminium. They found that boiling heat transfer coefficient enhances for all three heater surfaces with increasing concentration of copper nanoparticles in the prepared nanofluids, roughness of surfaces and depends on the material of surface. They observed that critical
heat flux increases with increasing Cu nanoparticle concentration and displays a maximum enhancement of ~60% for nanofluid containing 0.5%wt of copper. The observed CHF enhancement is attributed to the increased surface roughness of the heating wire due to the formation of peaks and valleys on the wire surface.

Available data were obtained for thin wires and flat plates. None of the experimental work was conducted with use of tubes. But, it is well known – from experimental as well as theoretical studies, that critical heat flux in pure, base liquids is strongly dependent on heater geometry [45]. The main aim of the proposed study is therefore recognition of the phenomena accompanying nucleate boiling crisis of selected nanofluids during boiling on horizontal tubes of various outside diameters. Of particular interest is impact of contact angle and tube diameter on the value of critical heat flux. The results obtained should give more light on the nature of nucleate boiling crisis and will serve as a basis for future theoretical modeling of the nucleate boiling crisis.

2. EXPERIMENT

2.1 Preparation and characterization of nanofluids

In the present study Al_2O_3, TiO_2 and Cu (Fig.1) were used as nanoparticles while distilled, deionized water was applied as a base fluid. Alumina (Al_2O_3), titania (TiO_2) and copper (Cu) nanoparticles, of spherical form have diameter from 5 nm to 250 nm. Their mean diameter was estimated to be 47 nm according to the manufacturer (Sigma-Aldrich Co.). Dispersants were not used to stabilise the suspension. Ultrasonic vibration was used for 30-60 minutes in order to stabilise the dispersion of the nanoparticles. Nanoparticles were tested at the concentration of 0.01%, 0.1%, and 1% by weight. The pH of nanofluids was ca. 7. All tests were performed under atmospheric pressure.

Fig. 2 shows the SEM photographs of Al_2O_3 and TiO_2 nanoparticle suspensions with the concentration of 0.01%. The experimental results showed that the stability of nanoparticle suspensions were good and during the test run, nanoparticle suspensions could maintain good uniformity.

2.2. Experimental apparatus and procedure

Figure 3 shows the schematic diagram of the experimental apparatus. The test chamber consisted of a cubical vessel made of stainless steel with inside dimensions of 150 x 150 x 250 mm. The horizontal stainless steel tubes having 1.6 mm and 3 mm of outside diameter and 0.6 mm wall thickness formed test heater. The effective length of the test tube was 180 mm. The ends of primary heater are soldered to short cooper cylindrical ends to minimize any additional electrical resistance. The test specimens were heated by using the tubes themselves as resistance heaters. The outside surface temperature, t_o, used for wall superheat determination was obtained as an analytical solution of the one-dimensional, steady-state heat conduction equation with uniform heat generation in the tube wall as:

$$t_o = t_i + \frac{U_t I_t}{4\pi\lambda L}\left[\frac{2\ln(D_o/D_i)}{(D_o^2/D_i^2)-1}-1\right] \quad (1)$$

where: U_t [V] – voltage drop, I_c [A] – current, D_o [m] – outside tube diameter, D_i [m] – inside tube diameter, L [m] – active length of a tube. The temperature of the inside surface of the test tube, t_i, was measured using a single thermocouple that displays an average temperature of the inside surface. The hot junction of the thermocouple was placed on the centre line of the tube at the midpoint of the test section. The wall superheat was calculated as

$$\Delta T = t_o - t_f \quad (2)$$

where t_f was calculated as the arithmetic mean of four measured fluid temperatures (Fig. 3). The heat flux was calculated as

$$\dot{q} = \frac{\dot{Q}}{A} = \frac{U_t I_t}{\pi D_o L} \quad (3)$$

Mean heat transfer coefficient was calculated as

$$\alpha = \frac{\dot{q}}{\Delta T} \quad (4)$$

The uncertainties of the measured and calculated parameters are estimated by mean-square method. The experimental uncertainty of heat flux was estimated as follows:

$$\Delta\dot{q} = \sqrt{\left(\frac{\partial\dot{q}}{\partial U_t}\Delta U_t\right)^2 + \left(\frac{\partial\dot{q}}{\partial I_t}\Delta I_t\right)^2 + \left(\frac{\partial\dot{q}}{\partial D_o}\Delta D_o\right)^2 + \left(\frac{\partial\dot{q}}{\partial L}\Delta L\right)^2} \quad (5)$$

where the absolute maximal measurement errors of the voltage drop ΔU_t, current ΔI_t, outside tube diameter ΔD_o and active length of a tube ΔL are 0,248 V, 1,57 A, 0.02 mm, and 4 mm, respectively. So, the maximum overall experimental limits of error for heat flux extended from ±4.3% for maximum heat flux up to ±30.6% for minimum heat flux. The soldering of the tubes at both ends adds uncertainty to the length of the whole tube and attributes to the largest uncertainty in the heat flux.
The experimental uncertainty for the average heat transfer coefficient is calculated as

$$\Delta\alpha = \sqrt{\left(\frac{\partial\alpha}{\partial\dot{q}}\Delta\dot{q}\right)^2 + \left(\frac{\partial\alpha}{\partial\Delta T}\delta T\right)^2} \quad (6)$$

where the absolute measurement error of the wall superheat, δT, estimated from the systematic error analysis equals ±0.2 K. The maximum error for average heat transfer coefficient was estimated to ±31%.

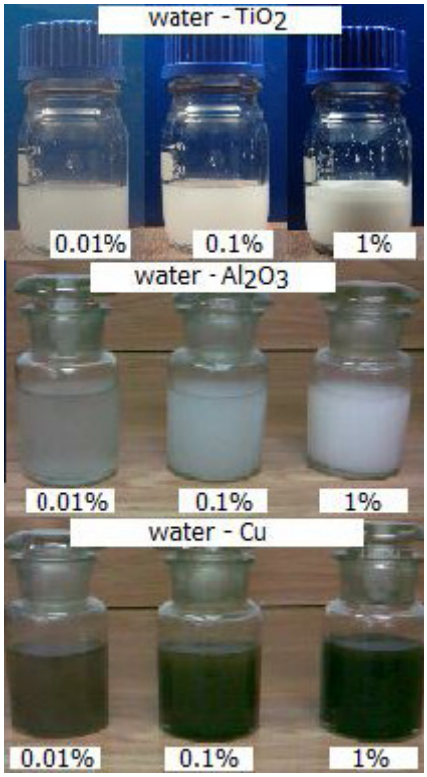

Fig. 1. Tested nanofluids

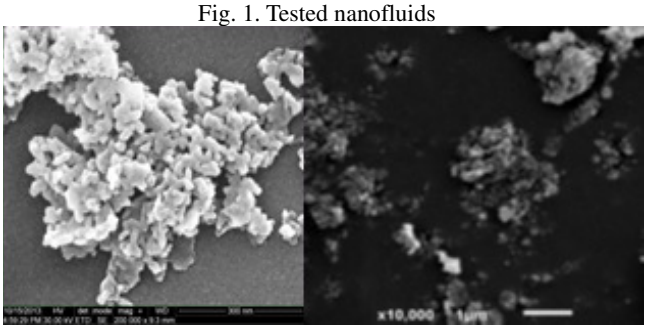

Fig. 2. SEM images of water-Al_2O_3 and water-TiO_2 nanofluids (0.01%)

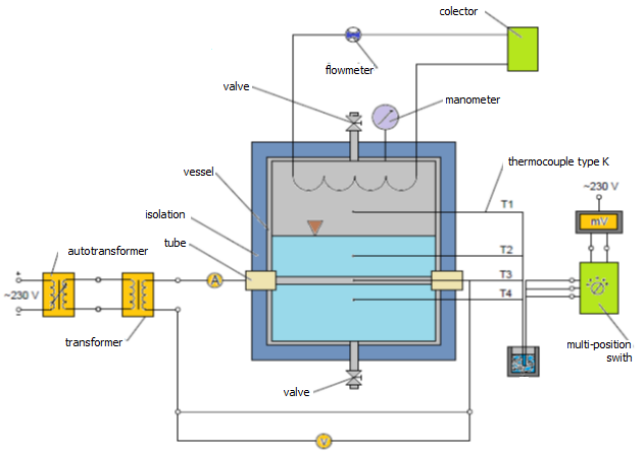

Fig. 3. Schematic diagram of the experimental apparatus

3. RESULTS AND DISCUSSION

Figure 4 and Fig. 5 show boiling curves and heat transfer coefficient, respectively, for water-Al_2O_3 nanofluid on stainless steel tube having 1.6 mm outside diameter at atmospheric pressure for three tested nanoparticle concentrations, i.e. 0.01%, 0.1% and 1%. The addition of nanoparticles Al_2O_3 results in dramatic heat transfer degradation. Moreover, the heat transfer coefficient decreases with nanoparticle concentration increase, particularly for higher heat flux. Present results for distilled water display satisfactory agreement with predictions obtained with Cooper's correlation [46] within the whole range of heat flux investigated.

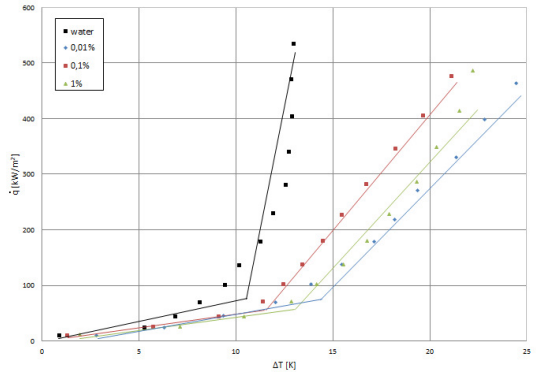

Fig. 4. Boiling curves for water-Al_2O_3 nanofluid on stainless steel tube (D_o = 1.6 mm)

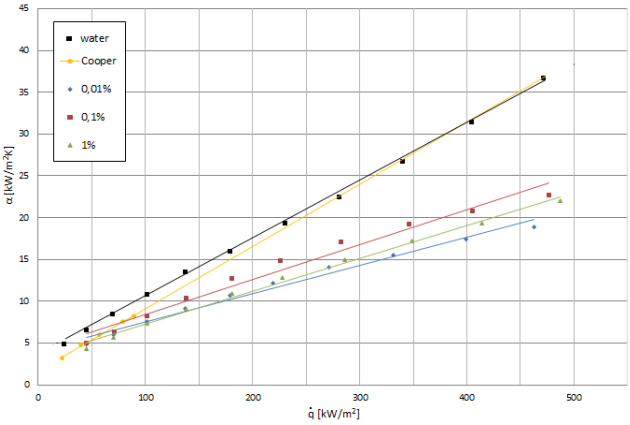

Fig. 5. Boiling heat transfer coefficient vs. heat flux for water-Al_2O_3 nanofluid on stainless steel tube (D_o = 1.6 mm)

Figure 6 and Fig. 7 show boiling curves and heat transfer coefficient, respectively, for water-TiO_2 nanofluid on stainless steel tube having 3 mm outside diameter at atmospheric pressure for three tested nanoparticle concentrations, i.e. 0.01%, 0.1% and 1%. As it seen in Fig. 6 and Fig. 7 that addition of even small amount of nanoparticles inhibits heat transfer in comparison with boiling of distilled water. Heat transfer coefficient decreases with nanoparticle concentration increase (Fig. 7), and boiling curves are shifted right, towards higher wall superheats (Fig. 6).

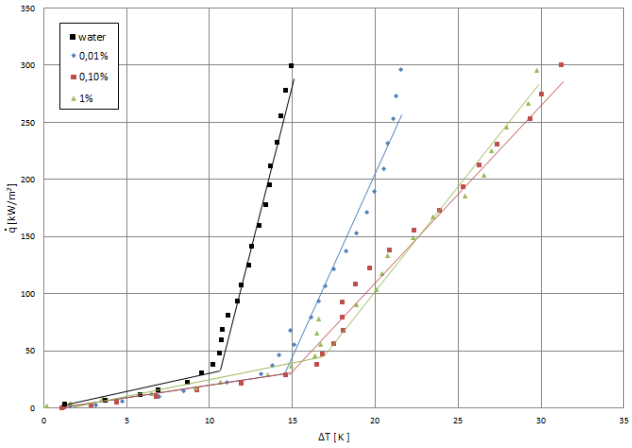

Fig. 6. Boiling curves for water-TiO_2 nanofluid for three tested nanoparticle concentrations, i.e. 0.01%, 0.1% and 1% on stainless steel tube (D_o = 3 mm)

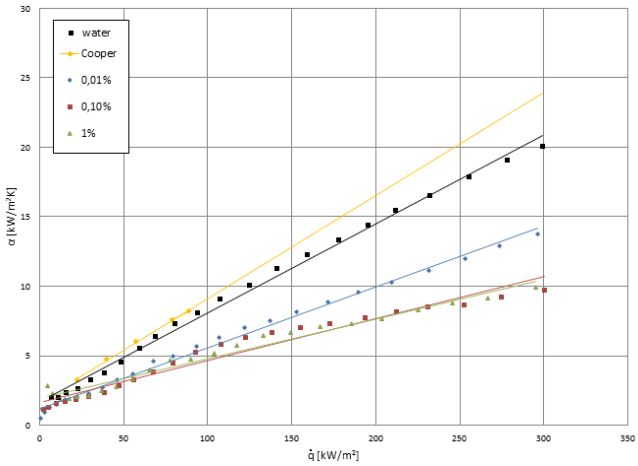

Fig. 7. Boiling heat transfer coefficient vs. heat flux for water-TiO_2 nanofluid for three tested nanoparticle concentrations, i.e. 0.01%, 0.1% and 1% on stainless steel tube (D_o = 3 mm)

Figure 8 shows boiling curves for discrete nucleate boiling and fully developed nucleate boiling regimes for water-Al_2O_3, water-TiO_2 and water-Cu nanofluids on stainless steel tube having 1.6 mm outside diameter at atmospheric pressure for nanoparticle concentration of 0.01%. Boiling curves are shifted right, towards higher wall superheats what indicates a dramatic heat transfer degradation As it seen in Fig. 9 the corresponding heat transfer coefficient is the highest for water-Al_2O_3 nanofluid and the lowest for water-TiO_2 nanofluid.

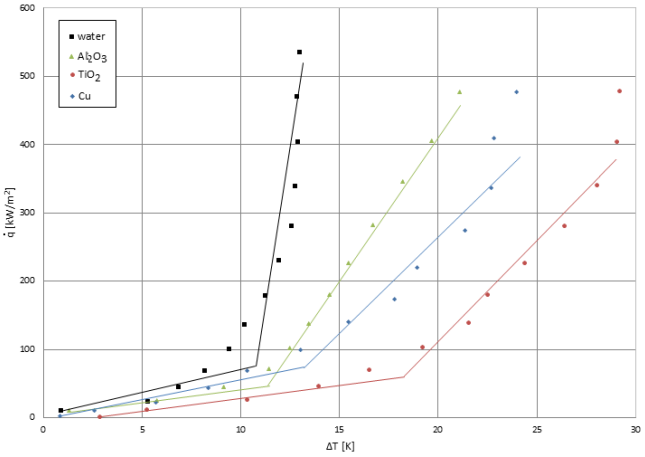

Fig. 8. Boiling curves for water-Al_2O_3, water-TiO_2 and water-Cu nanofluids with nanoparticle concentration of 0.01% on stainless steel tube (D_o = 1.6 mm)

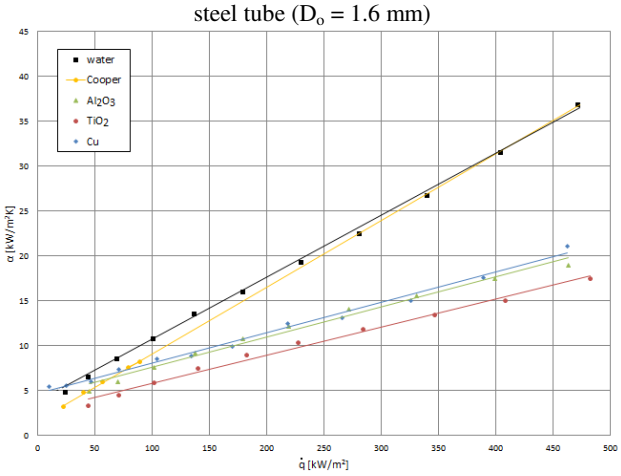

Fig. 9. Boiling heat transfer coefficient vs. heat flux for water-Al_2O_3, water-TiO_2 and water-Cu nanofluids for nanoparticle concentration of 0.01% on stainless steel tube with outside diameter of 1.6 mm

Independent of the nanoparticle material and nanoparticle concentration, enhancement factor k_{eff}, defined as a ratio of heat transfer coefficient for nanofluid to the heat transfer coefficient for distilled water at the same wall superheat, decreases with heat flux increase – Fig. 10.

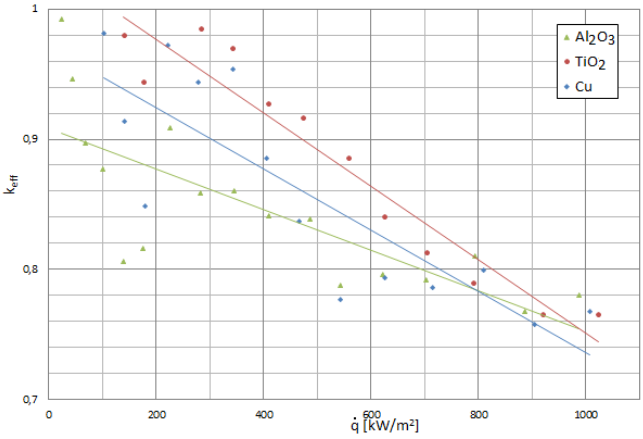

Fig. 10. Enhancement factor for water-TiO_2, water-Al_2O_3 and water-Cu nanofluids with 0.01% nanoparticle concentration boiling on the stainless steel tube (D_o = 1.6 mm)

Figure 11 shows boiling curves and CHF region for distilled water on stainless steel tube of 1.6 mm and 3 mm outside diameter. The recorded burnout values (1075 kW/m^2 and 1377 kW/m^2, respectively) are very close to the predictions made by use of the Kutateladze-Zuber (1325 kW/m^2) and Haramura-Katto (1050 kW/m^2) correlations and seem to confirm hydrodynamic nature of the first boiling crisis [47].

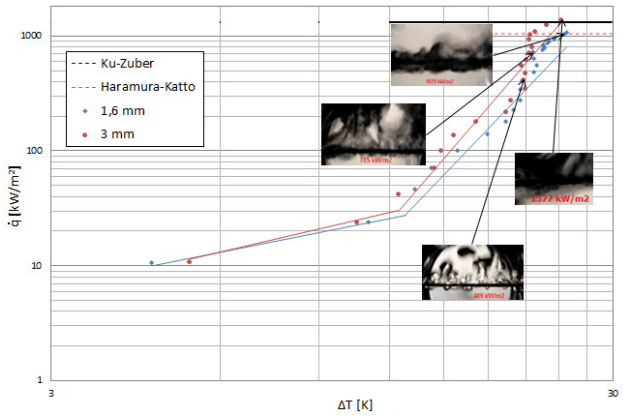

Fig. 11. Boiling curves and CHF values for deionized water on stainless steel tube (D_o = 1.6 and D_o =3 mm)

Figure 12 depicts the boiling curves for water-Al_2O_3, water-TiO_2 and water-Cu nanofluids on stainless steel tube at atmospheric pressure for nanoparticle concentration of 0.01%. and Fig. 13 experimental points for fully developed nucleate boiling. The recorded burnout values for water-Al_2O_3 and water-TiO_2 are the largest. Addition of Al_2O_3 and TiO_2 nanoparticles resulted in 171% (1843.6 kW/m^2) and 176% (1889.7 kW/m^2) enhancement of CHF during boiling of water-Al_2O_3 and water-TiO_2 nanofluids on stainless steel tube compared to that of pure water, respectively. The recorded burnout value for water-Cu nanofluid (1354.2 kW/m^2) is very close to the value of pure water.

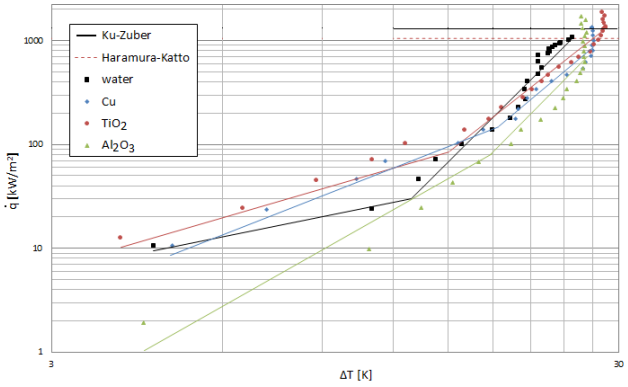

Fig. 12. Boiling curves and CHF values for deionized water and water-Al_2O_3, water-TiO_2 and water-Cu nanofluids on stainless steel tube (D_o = 1.6 mm)

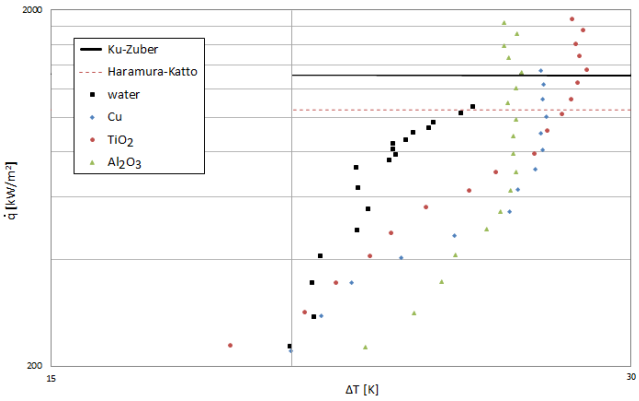

Fig. 13. CHF values for deionized water, water-Al_2O_3, water-TiO_2 and water-Cu nanofluids on stainless steel tube (D_o = 1.6 mm)

As it was already reported in the literature [14, 31-33, 37], a kind of nanocoating has been detected on the tube surface after boiling experiment. Figure 14 and Fig. 15 illustrate Al_2O_3 and TiO_2 nanocoatings developed on the tube surface with outside diameter of 1.6 mm, respectively. The SEM images of the nanocoatings taken with small magnification (Fig. 14a and Fig 15a) show no distinctive differences in the coating structures. The nanocoatings have a patchy non-uniform consistency. Because of strong effect of the absorption of electrons it was impossible to take SEM images of the Al_2O_3 nanocoating with magnification greater than 10000x (Fig. 14b). Contrary to Al_2O_3 nanocoating, TiO_2 nanocoating displayed higher electrical conductivity, so it was possible to take SEM images with magnification of 100000x and it is seen that the nanocoating is very porous and regular.

a)

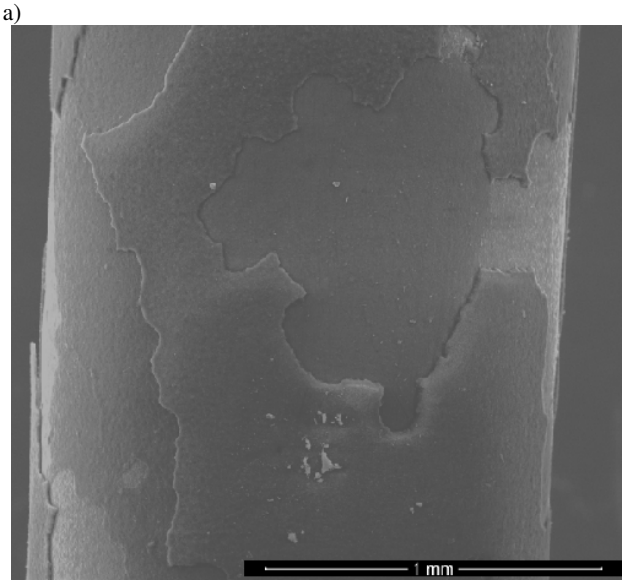

b)

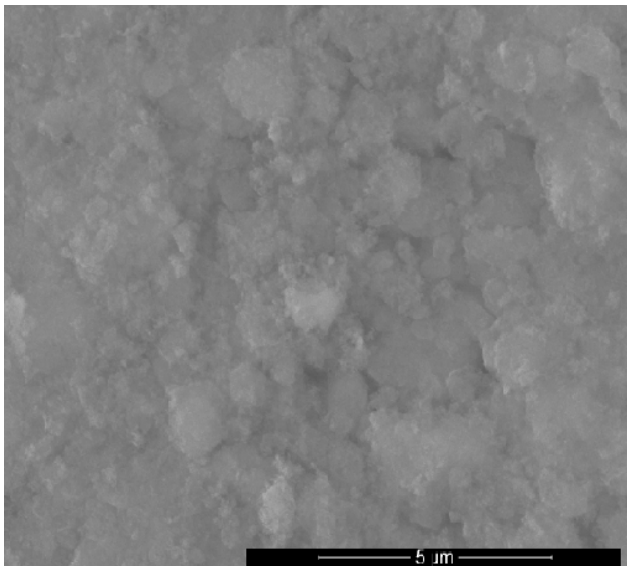

Fig. 14. SEM images of the tube surface with nanocoating developed during boiling of water-Al_2O_3(0.01%vol.) nanofluid; a) magnification (75x), b) magnification (10000x)

a)

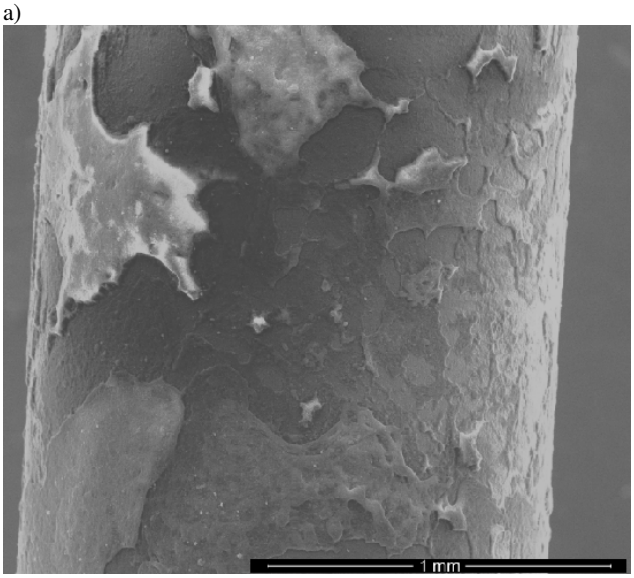

b)

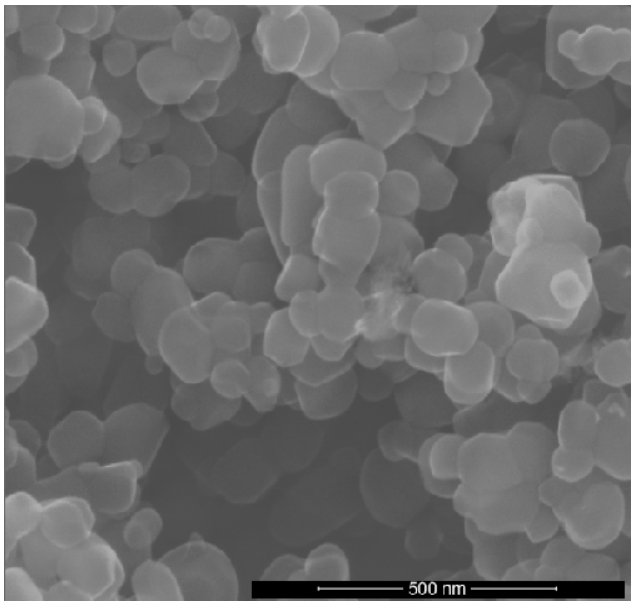

Fig. 15. SEM images of the tube surface with nanocoating developed during boiling of water-TiO_2(0.01%vol.) nanofluid; a) magnification (75x), b) magnification (100000x)

There is a consensus that CHF enhancement during nanofluid pool boiling is related to the formation of a nanocoating on the heating surface. The fact that the microlayer evaporation underneath the bubble attached to the heater surface is responsible for the deposition of the nanoaparticles (nanocoating) is unquestioned [8,11,31]. However, the role of the nanocoating in CHF progress is still under study. Some researchers point out that the nanocoating significantly improved the surface wettability and as a result CHF enhancement is observed [14,39]. The role of disjoining pressure is emphasized [48, 49] emphasized. Recently, the relation between the CHF enhancement and Taylor instability as well as Helmholtz instability is studied [50-52]. Inhibition of the irreversible growth of a hot/dry spot due to increased stability of the evaporating microlayer underneath a bubble growing on a nanocoating is supposed to improve CHF [35].

4. CONCLUSIONS

Independent of the nanoparticle concentration and material (Al_2O_3, TiO_2 and Cu), addition of nanoparticles caused dramatic degradation of pool boiling heat transfer on smooth, horizontal stainless steel tube.

Enhancement factor for all tested nanofluids (water-TiO_2, water-Al_2O_3 and water-Cu) decreases with heat flux increase.

Critical heat flux obtained for distilled water on stainless steel tube agrees satisfactory with predictions obtained by use of the Kutateladze-Zuber and Haramura-Katto correlations.

Addition of Al_2O_3 and TiO_2 nanoparticles resulted in dramatic enhancement of CHF during water-Al_2O_3 and water-TiO_2 nanofluids boiling on stainless steel tube compared to that of pure water. The recorded burnout value for water-Cu nanofluid was very close to the value of pure water.

Nanocoatings of different structures were detected on the tube surface after CHF boiling experiment for all three tested nanofluids

REFERENCES

1. S. Lee, U.S. Choi, Li S., Eastman J.A., Measuring thermal conductivity of fluids containing oxidie nanoparticles, ASME

Journal of Heat Transfer, vol. 121, pp. 280-289, 1999.
2. J.T. Cieśliński, T. Kaczmarczyk T., Pool boiling of water-Al_2O_3 and water-Cu nanofluids on horizontal smooth tubes. *Nanoscale Research Lett*., 2011, doi:10.1186/1556-276X-6-220 - ISSN 1556-276X.
3. J.T. Cieśliński, T. Kaczmarczyk T., Pool boiling of water-Al_2O_3 and water-Cu nanofluids on porous coated tubes. *Heat Transfer Engineering* (available on-line in October 2014, hard copy – March 2015)
4. S.M. You, J.H. Kim, K.H. Kim, Effect of nanoparticles on critical heat flux of water in pool boiling heat transfer, *Applied Physics Letter, vol.* 83, pp. 3374–3376, 2003.
5. P. Vassallo, R. Kumar, S. D'Amico, Pool boiling heat transfer experiments in silica-water nanofluids, *International Journal of Heat and Mass Transfer*, vol. 47, pp. 407–411, 2004.
6. N. Dinh, J. Tu, T. Theofanous, Hydrodynamic and physico-chemical nature of burnout in pool boiling, 5th *International Conference on Multiphase Flow*, Yokohama, paper No. 296 (CD-ROM), 2004.
7. G. Moreno, S.J. Oldenburg, S.M. You, J.H. Kim, Pool boiling heat transfer of alumina-water, zinc oxide-water and alumina-water-ethylene glycol nanofluids, Paper no. HT2005-72 375 pp. 625-632, http://dx.doi.org/10.1115/HT2005-72375.
8. I.C. Bang and S.H. Chang, Boiling heat transfer performance and phenomena of Al_2O_3–water nanofluids from a plain surface in a pool. *International Journal of Heat and Mass Transfer*, vol. 48, pp. 2407–2419, 2005.
9. D. Milanova, R. Kumar, Role of ions in pool boiling heat transfer of pure and silica nanofluids. Applied Physics Letters 2005, 87:233107.
10. J.E. Jackson, B.V. Borgmeyer, C.A. Wilson, P. Cheng, J.E. Bryan, Characteristics of Nucleate Boiling with Gold Nanoparticles in water. In IMECE2006; November 5-10, 2006; Chicago, Illinois, USA, 2006.
11. H. Kim, J. Kim, M.H. Kim, Effect of nanoparticles on CHF enhancement in pool boiling of nano-fluids, *International Journal of Heat and Mass Transfer*, vol. 49, pp. 5070-5074, 2006.
12. H. Kim, J. Kim, M. Kim, CHF enhancement in pool boiling of water-TiO_2 nanofluids: effect of nanoparticle-coating on heating surface, *13th Int. Heat Transfer Conference*, Sydney, paper NAN-22 (CD-ROM), 2006.
13. S.J. Kim, I.C. Bang, J. Buongiorno, L.W. Hu, Effects of nanoparticle deposition on surface wettability influencing boiling heat transfer in nanofluids, *Applied Physics Letters*, vol. 89, pp. 153107, 2006.
14. S. Kim, I. Bang, J. Buongiorno, L. Hu, Surface wettability change during pool boiling of nanofluids and its effect on critical heat flux, *International Journal of Heat and Mass Transfer*, vol. 50, pp. 4105-4116, 2007.
15. M.R. Kashinath, Parameters affecting critical heat flux on nanofluids: heater size, pressure orientation and anti-freeze addition, MSc, University of Texas at Arlington, 2006.
16. D. Milanova, R. Kumar, S. Kuchibhatla, S. Seal, Heat transfer behavior of oxide nanoparticles in pool boiling experiment, *Int. Fourth International Conference on Nanochannels, Microchannels and Minichannels* (ICNMM2006); June 19-21, 2006; Limerick, Ireland. 2006.
17. H. Kim, J. Kim, M. Kim, Experimental study on CHF characteristics of water-TiO_2 nano-fluids, *Nuclear Engineering and Technology,* vol. 38, pp. 61-68, 2006.
18. H.D. Kim, M.H. Kim, Effect of nanoparticle deposition on capillary wicking that influences the critical heat flux in nanofluids, *Applied Physics Letters,* vol. 91, pp. 014104, 2007.
19. H. Kim, J. Kim, M. Kim, Experimental studies on CHF characteristics of nano-fluids at pool boiling, *International Journal of Multiphase Flow*, vol. 33, pp. 691-706, 2007.
20. Z. Liu, J. Xiong, R. Bao, Boiling heat transfer characteristics of nanofluids in a flat heat pipe evaporator with micro-grooved heating surface, *International Journal of Multiphase Flow*, vol. 33, pp. 1284-1295, 2007.
21. J. Coursey and J. Kim, Nanofluid boiling: The effect of surface wettability, *International Journal of Heat and Fluid Flow*, vol. 29, pp. 1577-1585, 2008.
22. Z. Liu and L. Liao, Sorption and agglutination phenomenon of nanofluids on a plain heating surface during pool boiling, *International Journal of Heat and Mass Transfer*, vol. 51, pp. 2593-2602, 2008.
23. D. Milanova and R. Kumar, Heat transfer behavior of silica nanoparticles in pool boiling experiment. ASME *Journal of Heat Transfe*, vol. 130, pp. 042401, 2008.
24. M.N. Golubovic, H.D. Madhawa Hettiarachchi, W.M. Worek, W.J. Minkowycz, Nanofluids and critical heat flux, experimental and analytical study, *Applied Thermal Engineering*, vol. 29, pp. 1281-1288, 2009.
25. B. Jo, P.S. Jeon, J. Yoo, H.J. Kim, Wide range parametric study for the pool boiling of nanofluids with a circular plate heater, *Journal of Visualization,* vol. 12, pp. 37-46, 2009.
26. R. Kumar and D. Milanova, Effect of surface tension on nanotube nanofluids, *Appl. Physics Lett.,* vol. 94, 073107, 2009.
27. H. Kim, M. Kim, Experimental study of the characteristics and mechanism of pool boiling CHF enhancement using nanofluids, *Int.J. Heat Mass Transfer*, vol. 45, pp. 991-998, 2009.
28. K.J. Park, D. Jung, S.E. Shim, Nucleate boiling heat transfer in aqueous solutions with carbon nanotubes up to critical heat fluxes, *Int. J. Multiphase Flow*, vol. 35, pp. 525-532, 2009.
29. H. Kim, G. DeWitt, T. McKrell, J. Buongiorno, L.W. Hu, On the quenching of steel and zircaloy spheres in water-based nanofluids with alumina, silica and diamond nanoparticles, *Int. Journal of Multiphase Flow*, vol. 35, pp. 27-438, 2009.
30. R. Kathiravan, R. Kumar, A. Gupta, R. Chandra, Preparation and pool boiling characteristics of copper nanofluids over a flat plate heater, *International Journal of Heat and Mass Transfer*, vol. 53, pp. 1673-1681, 2010.
31. S.M. Kwark, R. Kumar, G. Moreno, J. Yoo, S.M. You, Pool boiling characteristics of low concentration nanofluids, *Int. Journal of Heat and Mass Transfer*, vol. 53, pp. 972-981, 2010.
32. S.M. Kwark, G. Moreno, R. Kumar, H. Moon, S.M. You, Nanocoating characterization in pool boiling heat transfer of pure water, *Int. J. Heat Mass Transfer*, vol. 53, pp. 4579-4587, 2010.
33. S.M. Kwark, M. Amaya, R. Kumar, G. Moreno, S.M. You, Effects of pressure, orientation, and heater size on pool boiling of water with nanocoated heaters, *International Journal of Heat and Mass Transfer*, vol. 53, pp. 5199-5208, 2010.
34. Z.H. Liu, X.F. Yang, J.G. Xiong, Boiling characteristics of carbon nanotube suspensions under sub-atmospheric pressures, *Int. J. Thermal Sciences,* vol. 49, pp. 1156-1164, 2010.
35. H. Kim, H.S. Ahn, M.H. Kim, On the mechanism of pool boiling critical heat flux enhancement in nanofluids, ASME *Journal of Heat Transfer*, vol. 132, pp. 061501, 2010.
36. S.D. Park, S. Won Lee, S. Kang, I.C. Bang, J.H. Kim, H.S. Shin, D.W. Lee, D. Won Lee, Effects of nanofluids containing graphene/graphene-oxide nanosheets on critical heat flux, *Applied Physics Letters*, vol. 97, pp. 023103, 2010.
37. B. Truong, L.W. Hu, J. Buongiorno, T. McKrell, Modification of sandblasted plate heaters using nanofluids to enhance pool boiling critical heat flux, *International Journal of Heat and Mass Transfer*, vol. 53, pp. 85-94, 2010.
38. R. Kathiravan, R. Kumar, A. Gupta, R. Chandra, Preparation and pool boiling characteristics of copper nanofluids

over a flat plate heater, *Heat Transfer Engineering*, vol. 33, pp. 69-78, 2012.
39. E.J. Park, S.D. Park, I.C. Bang, Y.B. Park, H.W. Park, Critical heat flux characteristics of nanofluids based on exfoliated graphite nanoplatelets (xGnPs), *Materials Letters,* vol. 81, pp. 193–197, 2012.
40. T. Lee, J.H. Lee, Y.H. Jeong, Flow Boiling CHF Characteristics of Magnetic Nanofluid under the Magnetic Field Condition, *Proceedings of ICAPP*, Paper No. KF129, 2013.
41. J.H. Lee, T. Lee, Y.H. Jeong, Experimental investigation on the CHF enhancement of pool boiling using water-based nanofluid at higher pressure, *Proc. of ICAPP*, Paper No. 131, 2013.
42. S.C. Hiswankar, J.M. Kshirsagar, Determination Of Critical Heat Flux In Pool Boiling Using ZnO Nanofluids, *Int. Journal of Engineering Research & Technology, v*ol. 2 Issue 7, 2013.
43. E. Park, I. Bang, H. Park, Critical heat flux (CHF) enhancement of the nanofluids by the electrical explosion of a wire in liquids, *Nanotech*, vol. 2, pp. 353 – 356, 2012.
44. Kole, Madhusree, T.K. Dey, Pool Boiling Heat Transfer and Critical Heat Flux Enhancement of Copper Nanoparticles Dispersed in Distilled Water, *Journal of Nanofluids*, vol. 3, Number 2, pp. 85-96(12), 2014.
45. Lienhard J. H., Dhir V. K.: Hydrodynamic prediction of peak pool-boiling heat fluxes from finite bodies. Transactions ASME. J. of Heat Transfer, vol. 95, 152–158, 1973.
46. M.G. Cooper, Heat Flow in Saturated Nucleate Pool Boiling– A Wide-Ranging Examination Using Reduced Properties, *Advances in Heat Transfer*, vol. 16, pp. 157-239, 1984.
47. J.T. Cieśliński, Modelling of nucleate pool boiling. Gdańsk, Wyd. P. Gdań, 2005 (in Polish).
48. K. Sefiane, J. Skilling, J. MacGillivray, Contact line motion and dynamic wetting of nanofluid solutions. *Advances in Colloid and Interface Science*, Vol. 138, pp. 101–120, 2008.
49. D. Wen, Mechanisms of thermal nanofluids on enhanced critical heat flux (CHF), *International Journal of Heat and Mass Transfer*, vol. 51, pp. 4958–4965, 2008.
50. S.D. Park, I.Ch. Bang, Investigation of mechanism on critical heat flux for nanofluid during pool boiling based on Taylor instability, *8th Int. Conf. on Multiphase Flow, ICMF, 2013*, Jeju, Korea, 2013.
51. W.R. Lee, W.S. Han, J.Y. Lee, Effect of flow instability on pool boiling and CHF of thin flat plate heater PCB, 8th *Int. Conf. on Multiphase Flow, ICMF*, 2013, Jeju, Korea, 2013.
52. R. Chen et al., Nanowires for Enhanced Boiling Heat Transfer, *Nano Lett.,* Vol. 9, No. 2, pp. 548-553, 2009.